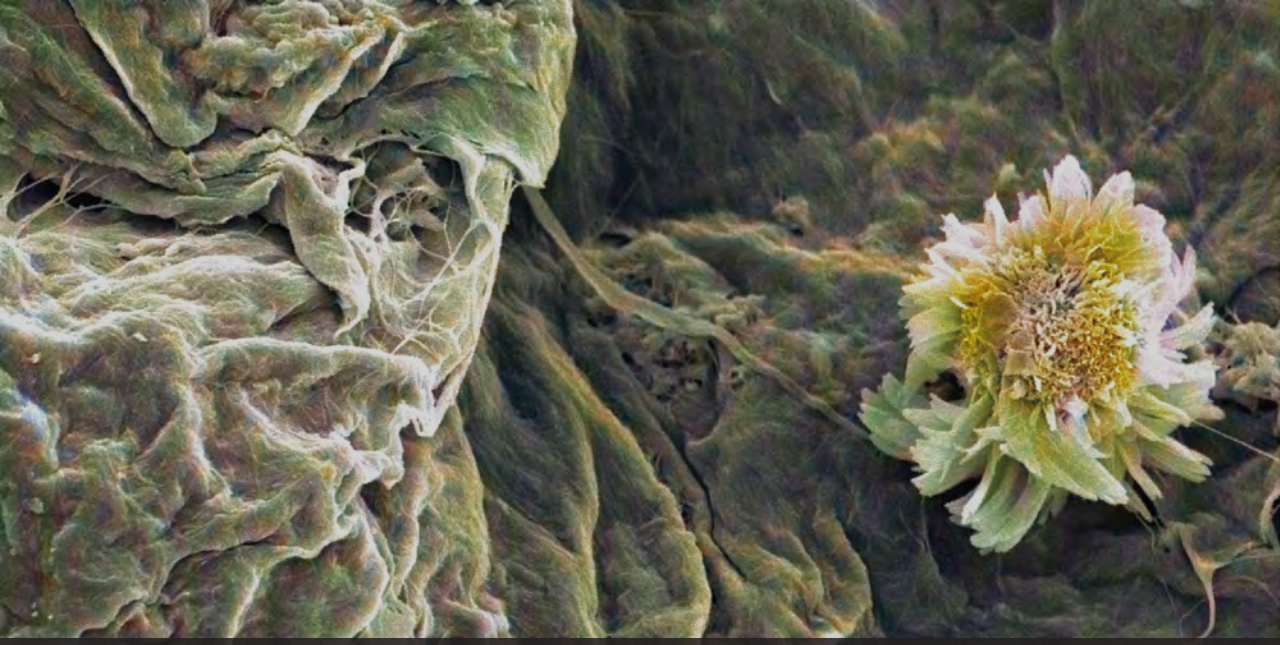

WATER RESISTANCE IMPROVEMENT OF BIOMINERALIZED BACTERIAL CELLULOSE WITH BIO-BASED COATINGS

by Maxim Velli

WATER RESISTANCE IMPROVEMENT OF BIOMINERALIZED BACTERIAL CELLULOSE WITH BIO-BASED COATINGS

BACHELOR THESIS

By

Maxim VELLI

Delft University of Technology

Department of Bionanoscience
DELFT UNIVERSITY OF TECHNOLOGY

Science supervisor: Prof. dr. M.E. Aubin-Tam
Daily supervisor: I.H.M.S. Nettersheim, BSc

July 2022

ABSTRACT

The overwhelming concerns about the future of humanity due to pollution by and depletion of petroleum-based materials have led global organizations to emphasize the urgency of transitioning to more sustainable consumption and production of materials. However, regardless of the acute necessity to change our consumption habits, plastics' excellent mechanical and physical properties have put pressure on scientists to find competitive alternatives in the realm of more sustainable materials. One of such novel materials is biomineralized bacterial cellulose (BMBC). BMBC is produced through three bacterial fermentations and is composed of 40% biopolymers (bacterial cellulose (BC) and poly-gamma-glutamic acid) and 60% $MgCO_3/CaCO_3$. Currently, its high water-absorbent capacity forms a bottleneck for the scope of its potential applications, as water absorption leads to a loss in mechanical properties. In order to expand the scope of possible applications of this novel material, this study looks into methods of improving the water-resistant properties of BMBC. Three methods were selected as compatible with the biological nature of the BMBC production process: coating with potassium stearate, coating with a chitosan solution, and coating with a zein solution. The coatings' capacity to enhance the material's water resistance was evaluated by measuring the wettability of the surface and water-absorbing capacity of a coated BMBC sample. The robustness of the applied coatings was also examined using controlled abrasion of the surface. It was found that potassium stearate coating showed the highest ability to reduce the wettability of the material's surface, while chitosan yielded the best capacity for preventing water absorption. The obtained results highlight the potential for using ion-exchange mechanisms for surface grafting of BMBC and elucidate the complications in applying a uniform coating to the formulated material. As BMBC is a novel material, this study makes the first step in expounding ways to tweak the physical properties of this biological composite to fit the desired applications.

Contents

1

INTRODUCTION

1.1. MOTIVATION FOR THE PROJECT

THE overwhelming pressure for a transition away from petroleum-based materials, as lined out by the 12th Sustainable Development goal of the United Nations United Nations, 2020, has been catalyzing research into bio-based alternatives for various materials. A creative outlook on utilizing nature's resources is the driving power behind accomplishing this transition towards a world of materials with a more sustainable life cycle. However, inventing new materials is often challenging, especially considering the well-established and researched fine-tuning of all petroleum-based materials. This gap makes it a profoundly nuanced endeavor, which the scientific world has been trying to resolve.

As lined out in thorough reviews by Zhu et al., 2016 and Mohanty et al., 2018, the rigidity of the global market and lack of urgent regulation and policies causes the invention of new materials often becoming a matter of recreating materials with the same properties as those of plastics and other products of the petrochemical industry. This imposed facet of the transition towards more sustainable materials is often criticized. Still, these properties serve as a good reference point for novel materials aspiring to achieve widespread use similar to the current industry leaders.

It is challenging to find good combinations of mechanical and physical properties within bio-based materials. Mechanical properties, such as high tensile strength, toughness, and strain, and physical properties, such as thermostability, hydrophobicity, and permeability, rarely coexist in natural materials. Considering the lack of natural materials with a good combination of properties similar to plastics, scientists have given attention to producing novel composites with readily and plentifully available biological matter. For example, Yu et al., 2021 discusses an easily scalable self-assembly approach for producing biomineralized bacterial cellulose (BMBC) composite in the recently published paper. This material is synthesized through three fermentations, and it consists of microfibrillated bacterial cellulose (BC), poly-gamma-glutamic acid (PGA), and crystals of $CaCO_3$ and $MgCO_3$. The obtained material's mechanical properties resemble nacre and acrylonitrile butadiene styrene (ABS) plastic (see Table 1 in Yu et al., 2021 for a comparison). However, this material demonstrates some drawbacks in its physical properties.

One of the deficient properties is the high hydrophilicity of this material, which can be attributed to the high content (40%) of the very hydrophilic bacterial cellulose in the composite. When BMBC absorbs water, it loses its good mechanical properties and swells, which forms a restriction in the range of potential applications. In the original paper by Yu et al., 2021, BMBC is proposed for applications in furniture and protective garments due to its recyclability. The capacity to be recycled is valuable, but it is also essential to tune the material's water resistance properties according to the desired applications. In this report, different strategies for ameliorating water resistance properties of BMBC are discussed, and two such strategies, chitosan and potassium stearate coatings, are quantitatively evaluated.

1.2. STRUCTURE OF BIOMINERALISED BACTERIAL CELLULOSE

In order to conceptualize an adequate approach to improving the material's water resistance, it is crucial to understand the molecular structure of BMBC. As seen in the Scanning Electron Microscopy (SEM) picture of Figure 3.11e, the cellulose fibers, which make up 40% of the material, are wrapped along and around the spherical mineral crystals, which make up the other 60%. Assuming a uniform distribution of the two components in the bulk material, an untreated surface of a BMBC sample will readily absorb water, as bacterial cellulose can absorb up to 150x of its mass in water (Ji-Suk Jeong, 2012). However, since the water-insoluble $CaCO_3$ and $MgCO_3$ crystals are only dispersed in the bulk material, they do not provide any water-resistant properties. Therefore, the surface or the composition of BMBC must be modified to contribute to reducing the hydrophilicity of the composite.

1.3. UNDERSTANDING HYDROPHOBICITY

The example of lotus (*Nelumbo nucifera*) leaves can demonstrate the two main strategies for ensuring surface hydrophobicity, as described in Ensikat et al., 2011. Firstly, epicuticular waxes cover the leaves of this plant; these waxes are hydrophobic molecules and lower the surface energy of the leaf. Lowering the surface energy results in water molecules being more attracted to each other than to the molecules of the surface. Thus, water molecules stick together instead of wetting the material. Secondly, micropapillae cover the leaf's surface, which leads to the formation of a very rough structure on micro-and nanoscales, as seen in the SEM picture in Figure 1.1. Such microstructures lead to the inability of the water drop to come in contact with the surface of the material without overcoming a critical pressure, resulting in the preferential adherence of the water molecules to themselves. Therefore, the two main strategies that can be employed are successfully modifying the surface of BMBC to have lower surface energy or inducing the formation of such microstructures.

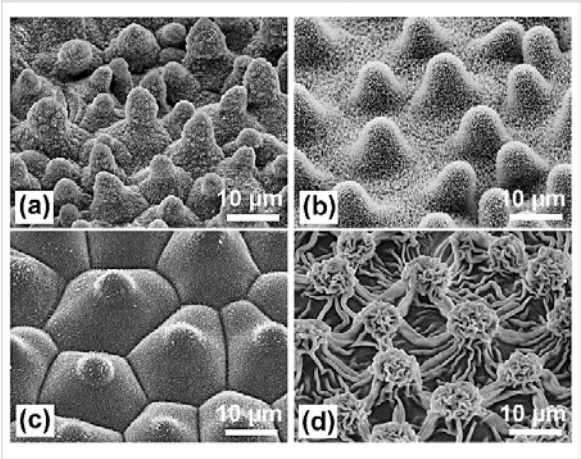

Figure 1.1: SEM micrograph of a lotus leaf surface, showing the micropapillae that contribute to surface roughness. Adapted from Ensikat et al., 2011

Quantification of hydrophobic properties of a material is crucial towards devising an optimal methodology for improving water resistance and clarifying the process by which the water resistance is improved. Several values can be reproducibly measured to act as a representation of a material's water resistance capacity. The four most popular methods are measuring the contact angle at which a drop of water is stable on the surface of the material(Fürstner et al., 2005, Nakajima et al., 2000); measuring the water absorption capacity upon immersion in water (Cabañas-Romero et al., 2020); measuring the angle at which a drop of water starts rolling off the surface (Nimittrakoolchai and Supothina, 2008, Bhushan et al., 2009); measuring material's water vapor permeability or sorption (Cabañas-Romero et al., 2020, Song and Rojas, 2013). In this project's scope, Water Contact Angle (WCA) and Water Absorption Capacity (WAC) have been used as measures for material's water resistance since measurements with water vapor required additional machinery and were not deemed immediately relevant to the proposed applications of BMBC.

In the context of WCA measurements, two thresholds are often considered significant: 90° and 150°. The prior signifies a surface with hydrophobic properties, whereas the latter signifies a superhydrophobic surface. Therefore, in the context of applied coatings, a WCA of at least 90° is necessary to instantiate the hydrophobicity of the material.

Additionally, the coating's performance against water "seeping through" is essential. The water drop should stay on the surface rather than "seep through" the coating and get absorbed. In order to investigate this matter, two measurements were conducted: a change in WCA after one minute on the material's surface and the time necessary for a water drop to disappear from the material's surface. The latter can either occur by evaporation from the surface, which signifies good water-resistant capacity, or by absorption into the material, which signifies poor coating performance.

Another value of interest for hydrophobic coatings is their capacity to withstand abrasion. Coating's resistance to abrasion is especially relevant for applications where the coating is expected to be touched or scratched, e.g., in domestic furniture. Therefore,

abrasion robustness was estimated by measuring the WCA before and after controlled abrasion of the coated material. By comparing the two, the effect of abrasion is quantified, and the robustness of the coating is evaluated.

1.4. CANDIDATES FOR ENSURING HYDROPHOBICITY

Due to the lack of studies on mitigating the water-absorbing properties of BMBC, literature on inducing hydrophobicity of (bacterial) cellulose was searched for methods that could be applied to the formulated biomineralized cellulosic material. Various approaches have been employed: both focused on lowering the material's surface energy and increasing the surface roughness. Some papers (Song and Rojas, 2013; Ji-Suk Jeong, 2012) demonstrate elaborate chemical functionalization of the cellulose surface to enhance hydrophobicity, while the scope of this research focuses on easily scalable and bio-based approaches. For example, Nyström et al., 2009 used principles of click chemistry with large molecules containing dense, aromatic groups to reduce surface wettability. The preference for more simplistic approaches to enhancing hydrophobicity allows for alignment with the core principles of the production process of BMBC, as shown by Yu et al., 2021.

Examples of compounds used for improving water- and oil resistance of paper and other cellulosic films include starch (Kansal et al., 2020), beeswax (Indriyati et al., 2020), polydopamine (X. Dong et al., 2019), soybean oil and ZnO (Cheng et al., 2017), zeolite (Zeng et al., 2017), betulin (Huang et al., 2021), PHBV (Andreotti et al., 2018), and many other biological or bio-derived molecules. However, many of these approaches utilize elaborate coating techniques, such as in works by Hahn et al., 2019 and Liu et al., 2015, requiring special equipment. The choice in favor of dip-coating and composite formulation was made to maintain the simplicity of BMBC formulation. Dip-coating can be conducted after drying the material to a sample of any size, which facilitates scalability. In addition, the biomineralization process allows for incorporating other molecules into the BMBC composite, which can be used to tune the mechanical and physical properties of the material. Finally, three compounds that fit the selection criteria on application simplicity and biological nature were chosen to be tested on their capacity to enhance the hydrophobicity of BMBC: potassium stearate, chitosan, and zein.

1.4.1. POTASSIUM STEARATE

The first strategy for qualitative evaluation of its hydrophobicity-enhancing capacity was dip-coating in potassium stearate. Potassium stearate is a salt of stearic acid obtained by a saponification reaction with potassium hydroxide. Stearic acid is a saturated long-chain fatty acid spanning over a hydrophobic tail of 18 carbon atoms. Stearic acid is a common component of various plant and animal fats, while cocoa and shea butter contain the most significant proportion of this fatty acid. Stearic acid is a renewable compound already finding applications in detergents, lubricates, and cosmetics and is being produced at an annual volume of at least 1600 kilotons (Coherent Marketing Insights, 2019). The availability and the market volume of stearic acid make it an attractive potential coating substrate for BMBC.

The approach towards coating BMBC with stearate was based on Hu et al., 2009, and it drew particular interest due to the proposed ion exchange mechanism that stearate anions experienced upon contact with $CaCO_3$. This mechanism was expected to highlight the benefits of the mineral composition of BMBC by utilizing the present mineral crystals for surface grafting, resulting in increased hydrophobicity (also see Figure 1.2). The role of calcium and magnesium ions in BMBC on the acquired hydrophobicity upon coating with stearate was studied by comparing the WCA of a stearate-coated BC sample to a stearate-coated BMBC sample. In addition, the influence of the kinetics of this ion exchange mechanism was studied by comparing dip-coating of BMBC in stearate to immersing BMBC in stearate for 15 minutes.

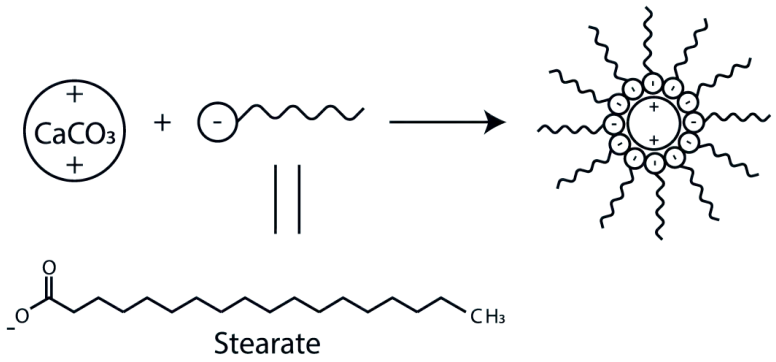

Figure 1.2: Hypothetical mechanism of stearate anions' adhesion to the surface of a calcium carbonate crystal. This mechanism is supposedly responsible for surface grafting of BMBC, which manifests into high surface hydrophobicity of the coated material. Adapted from Hu et al., 2009

1.4.2. CHITOSAN

The second molecule that was selected for quantitative analysis is chitosan. Chitosan is a linear hydrophobic polysaccharide that is produced by exposing chitin to an alkaline environment (see Figure 1.3 for molecular structure). Chitin is the second most abundant polysaccharide in nature after cellulose (Belgacem and Gandini, 2008), which makes chitosan an attractive candidate as a renewable and readily available substrate for hydrophobic coating. It also possesses antibacterial properties (Yilmaz Atay, 2019), consolidating the interest in integrating chitosan into the formulated BMBC material.

The incorporation of chitosan in a cellulosic material was based on the work by Fernandes et al., 2009, resulting in a method for creating a BMBC-chitosan composite. This composite was expected to possess enhanced hydrophobic and antibacterial properties, which would benefit the potential applications of this material. The incorporation of chitosan in the composite was also expected to change the mechanical properties of BMBC.

The second approach to employing chitosan to enhance BMBC hydrophobicity was dip-coating it in a chitosan solution. While chitosan is insoluble in water, it dissolves under weakly acidic conditions (Pardo-Castaño and Bolaños, 2019). Lactic acid and acetic acid are often used to induce protonation of the polysaccharide units, resulting in a charged molecule that dissolves in an aqueous acidic solution. Due to $CaCO_3$ and $MgCO_3$ in BMBC, the pH of the coating mixture should be kept as neutral as possible. This research used 1% acetic acid to dissolve chitosan in concentrations from 0.25% to 1.0%. No measurements on the maximal solubility of chitosan in acetic acid under such conditions are available, but this range was based on the methodology in Fernandes et al., 2009.

After applying chitosan coating to BMBC, the sample is dried, and, as the chitosan coating loses the liquid, a chitosan film is expected to form on the sample's surface. This film is expected to enhance the hydrophobicity of the surface using chitosan's natural hydrophobicity and by increasing the roughness of the surface (Ivanova and Philipchenko, 2012).

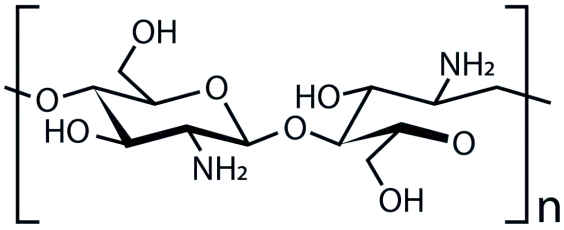

Figure 1.3: Molecular structure of chitosan

1.4.3. ZEIN

The third compound that was identified as a suitable substrate for enhancing the hydrophobic properties of BMBC was zein. This hydrophobic maize protein can be found in maize endosperm cells. It contains more than 50% of hydrophobic amino acids and has been employed in formulating nanomaterials with outstanding hydrophobic properties (Gianazza et al., 1977). Zein can also form various microstructures on the surface of materials when evaporation from this surface or the bulk of the material is induced (F. Dong et al., 2013). Results of the paper by Wan et al., 2017 led to a hypothesis that zein would induce the formation of such microstructures on the surface of BMBC, thereby increasing the roughness of the surface on a microscale. These microstructures would, in turn, decrease the surface's wettability and improve hydrophobicity.

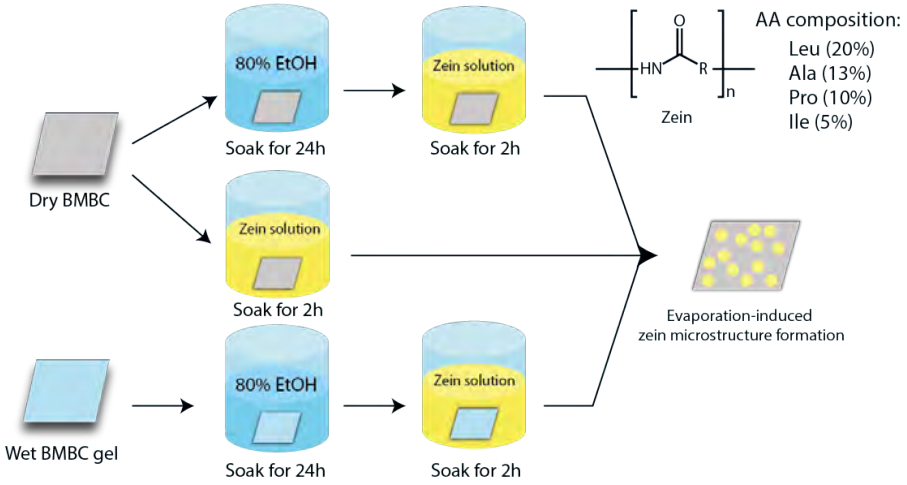

Figure 1.4: Three approaches to achieving microstructure formation on the surface of BMBC by using evaporation-induced microstructure formation of zein. The molecular structure and partial amino acid composition are also provided

Three different approaches were attempted to induce the formation of such microstructures: by immersing a dry BMBC sample in a zein-in-ethanol solution and letting it air-dry; by soaking dry BMBC in ethanol and then immersing it in zein-in-ethanol, after which the sample was air-dried; by solvent exchanging the water-saturated BMBC with ethanol, immersing in zein-in-ethanol and air-drying after (see Figure 1.4 for a visual representation of this methodology). The expected result was increased surface roughness and hydrophobicity of BMBC samples.

2

MATERIALS & METHODS

2.1. MATERIALS

FOR synthesis of potassium stearate, reagent grade (95%) stearic acid ($C_{17}H_{35}CO_2H$) and Potassium Hydroxide (KOH) pellets were obtained from Sigma Aldrich. Deionized (DI) water was used for preparation of all solutions and dilutions. Glacial acetic acid (Sigma Aldrich) was used to dissolve low molecular weight chitosan (Sigma Aldrich). Zein and sodium alginate were also obtained from Sigma Aldrich. An Avanti® high-speed centrifuge was used for dewatering the obtained BC and BMBC.

JEOL JSM 6010 LA Scanning Electron Microscope was used to observe the morphology of the (coated) samples. Gold-palladium sputter coating was applied at 20mA for 40s, after which the samples were loaded into the SEM for imaging. Images were taken in the secondary electron imaging (SEI) mode at 8 kV in vacuum.

2.2. PRODUCTION OF BIOMINERALISED BACTERIAL CELLULOSE

As described in the original work on the production of BMBC (Yu et al., 2021), a hierarchical self-assembly approach to producing biomineralized bacterial cellulose composites has been developed. This process encompasses three main steps that precede the recovery of bulk BMBC. These steps are briefly discussed in this subsection, but for a more thorough protocol, including media composition, refer to Yu et al., 2021. First, bacterial cellulose is produced by *Gluconacetobacter hansenii* during a fermentation that spans approximately two weeks. Upon the formation of the cellulosic pellicle, the fermentation is stopped, and the pellicle is harvested. This pellicle is then cut into smaller pieces, shredded using a kitchen blender, and microfibrillated using cellulase. Another necessary component for the following step is PGA, produced in a different fermentation by *Bacillus licheniformis*.

In contrast to the original paper, for all the samples prepared in the frame of this report, PGA fermentation broth was used instead of purified PGA. Upon obtaining the PGA broth and the microfibrillated bacterial cellulose, another fermentation that contains PGA, BC, urea, $CaCl_2$, and $MgCl_2$ is started, during which the process of formation of BMBC is

induced. *Sporosarcina pasteurii* enables the process of the formation of $CaCO_3$ crystals in bulk by converting urea into CO_3^- and NH_4^+. Calcium and magnesium ions form insoluble salts with CO_3^- resulting in crystal growth. PGA inhibits this growth, resulting in a more homogeneous distribution of crystal sizes and, therefore, more uniform mechanical properties of the biomineralized cellulosic composite. This fermentation takes place over 24h, after which the produced BMBC is harvested and centrifuged. After obtaining bulk BMBC, 0.5% w/w of sodium alginate is added to BMBC to obtain a 3D-printable ink.

2.2.1. POTASSIUM STEARATE SOLUTION PREPARATION

Potassium stearate was synthesized through a saponification reaction between stearic acid and potassium hydroxide: $KOH + C_{17}H_{35}CO_2H \rightarrow K{+}C_{17}H_{35}CO_2^- + H_2O$. This reaction was performed in a reflux condenser at 70°C under moderate agitation. First, KOH pellets were dissolved in water, after which stearic acid powder was added to the alkaline solution to start the reaction. Next, the chemicals were added in respective proportions to obtain a mother solution of 0.150M. This solution was then used to obtain diluted potassium stearate solutions of 0.002M, 0.005M, 0.015M, and 0.03M.

2.2.2. CHITOSAN SOLUTION PREPARATION

0.25%, 0.5%, 0.75% and 1.0% (w/v) chitosan solutions were prepared by adding a respective amount of chitosan to a 1% (v/v) acetic acid solution. Due to the viscosity of chitosan solutions under slightly acidic conditions, the solution was continuously vigorously stirred and maintained at 60°C for six hours to ensure full extension and dissolution of the chitosan fibers.

2.2.3. ZEIN SOLUTION PREPARATION

A 0.5% (w/v) solution of zein was prepared by dissolving the zein powder in a 80% (v/v) ethanol/water mixture. Zein contains up to 50% hydrophobic amino acids (Gianazza et al., 1977), so it readily dissolves in this mixture under slight stirring.

2.2.4. COATING WITH POTASSIUM STEARATE

Before coating, potassium stearate solutions were warmed up to 70°C under moderate stirring until the solution was transparent. At this temperature, the viscosity of the solution decreased, which ensured that the dipped sample did not get stuck in the solution. Moreover, decreased viscosity and higher temperature result in an optimal homogeneous distribution of stearate molecules in the solution. These conditions were hypothesized to be beneficial in facilitating the ion exchange of stearate between potassium and calcium in the BMBC.

Coating with potassium stearate was initially performed by picking up the sample with tweezers, immersing it fully into the solution for three seconds, and extracting it. Upon extraction, the sample was rinsed three times in DI water to remove the unadhered or excessively adhered stearate molecules. After rinsing, the samples were placed in a 24-well plate to dry under ambient conditions vertically for four days.

However, this dipping technique yielded very inconsistent results for WCA measurements (Figure 3.1). In order to improve the reproducibility and consistency of the experiment, this coating treatment was modified. The BMBC samples were immersed in a

potassium stearate solution at 70°C for 15 minutes under light stirring to allow a more uniform adhesion of stearate molecules onto the sample's surface. This method was based on forming PCC crystals with bound stearate, as described by Hu et al., 2009. Immersion of a BMBC sample in a stearate solution did not have a noticeable effect on the swelling of the sample, but further investigation of the optimal duration of this reaction is required.

2.2.5. COATING WITH CHITOSAN

Coating with chitosan solutions was performed at room temperature. The coating procedure included complete immersion of the BMBC samples into the viscous solutions of chitosan for three seconds, after which they were taken out with tweezers and dried under ambient conditions for four days. Initially, the samples were vertically dried, but this yielded inconsistent results for WCA measurements (see Figure 3.5). Presumably, the reason for that was the flow of the viscous solution to the lower part of the sample before a chitosan film could form uniformly on the surface. This was resolved by letting the samples dry horizontally on a grid to ensure ventilation. In this case, a difference in hydrophobic properties between the "upper" and "lower" sides of the dried samples was anticipated. However, upon obtaining results for the WCA measurements, both sides had similar hydrophobic properties.

2.2.6. COATING WITH ZEIN

The protocol for coating with zein was based on Wan et al., 2017. However, the specifics of the BMBC printable material, as elaborated on in the Discussion section, demanded some adjustments. In order to account for that, three different ways of coating BMBC samples with zein were attempted. The first included immersion of a dry BMBC sample in a 0.5% w/v zein in 80% ethanol solution for two hours statically at room temperature, after which the sample was air-dried for 24h. The second was performed by first immersing the dry BMBC sample in an 80% ethanol solution for 24h at room temperature. Then, it was moved into a 0.5% w/v zein in 80% ethanol solution for two hours and then air-dried for 24h. The third was performed with a wet BMBC sample that was immersed in an 80% ethanol solution for 24h at room temperature to allow for a solvent exchange of water with ethanol in the sample. After this, the ethanol-saturated sample was moved into a 0.5% w/v zein in an 80% ethanol solution for two hours, then air-dried for 24h.

2.3. WATER CONTACT ANGLE MEASUREMENTS

Hydrophobicity of BMBC or BC samples was evaluated by measuring the Water Contact Angle (WCA) in triplicates. WCA measurements were performed by letting a single drop of water (6 µL) fall from the tip of a micropipette onto the material's surface. An image of the contact point of the drop with the surface was taken synchronously. The images were taken using a macro camera. Four images of four drops were taken for each sample, two on one side and two on the reverse. The images were then analyzed with ImageJ Image Processing and Analysis Software (Schneider et al., 2012) software, using the Contact Angle (Brugnara, 2006) plugin. This software conducts a circle best fit to the shape of the drop on the surface, thereby providing information on the contact angle. An example for how such a fit is performed is displayed in Figure 2.1. For some measurements, an image

was taken directly after depositing the water drop, and for some - after leaving the drop on the surface for a given time (e.g., one minute).

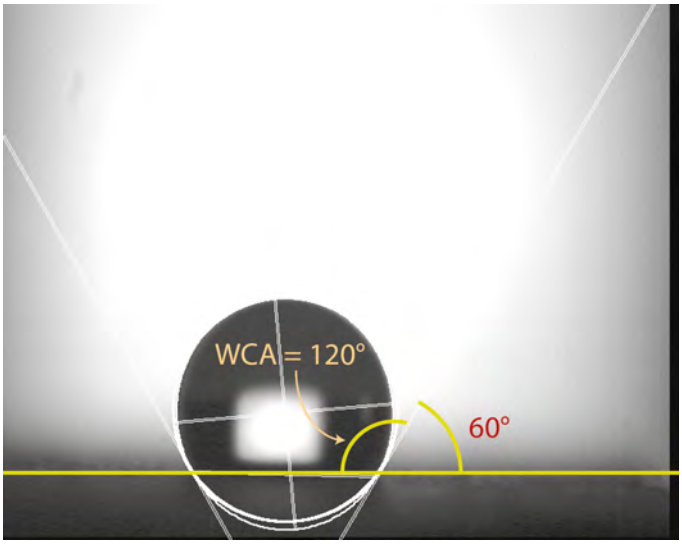

Figure 2.1: An example of how a best circle fit is performed by the Contact Angle plugin for ImageJ. The white lines are placed by the software and the yellow lines are supplementary to signify the relation of the measured angle to the WCA.

2.4. WATER ABSORPTION CAPACITY MEASUREMENTS

The Water Absorption Capacity (WAC) of the coated BMBC samples was determined in order to evaluate the capacity of the hydrophobic coating to prevent the swelling of material after submerging the sample into water. This method was adapted from Cabañas-Romero et al., 2020. Firstly, a dry ($\geqslant$ 4 days of drying under ambient conditions) sample was weighed, then the sample was submerged in DI water for 20h. Hereafter, the sample was taken out of the water, both sides wiped by a KIMTECH® precision wipe, and its mass measured.

2.5. ABRASION TESTING & SET UP

In order to test the robustness of the applied hydrophobic coating, the surface's hydrophobicity was tested after controlled abrasion of the sample. Abrasion was performed based on Veigel et al., 2017 and included applying a force of 2N onto a coated sample of 1.5x1.5cm and dragging for 30 cm along a sandpaper surface with a grain of 88 µm with a velocity of 10cm/s. Controlled abrasion was done using a 3D printer as a basis for the set-up that is depicted in Figure 2.2.

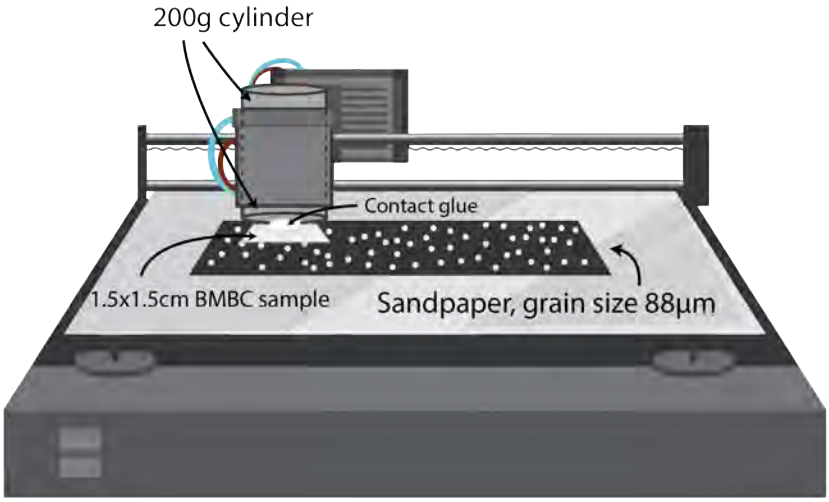

Figure 2.2: Set up for controlled abrasion of (coated) BMBC. The 3D printer head is used to control the velocity at 10cm/s. The 200g cylinder is loosely held by the head of the 3D printer to ensure that it moves along the horizontal axis but keeps applying pressure to the 1.5x1.5cm sample attached to the cylinder with contact glue. The grain size of sandpaper is 88µm.

2.6. STATISTICAL ANALYSIS

Statistical analysis was performed using the Statistical module of the SciPy library (Virtanen et al., 2020) for simple and paired T-tests. For pairwise Tukey tests, the Statsmodel library (Seabold and Perktold, 2010) was used. An alpha threshold of 0.05 was used in most cases unless otherwise stated within the context.

3

RESULTS

3.1. POTASSIUM STEARATE

Two ways of applying a potassium stearate coating to a BMBC sample were tested: immersing the sample for three seconds or 15 minutes. Figure 3.1 shows the WCA measurements' results for the two coating application methods. This figure compares the efficiency of the two methods and their relation to an uncoated negative control.

Samples immersed for 15 minutes in stearate solution yielded WCA higher than 90°C for all stearate concentration, and reaching as high as 136° for some samples at 0.03M stearate, which corresponds to high surface hydrophobicity. Furthermore, in comparison to the negative control, for which the mean WCA was 15°, the increase in mean WCA for a stearate concentration of 0.002M (mean WCA = 104.93°) was also significant ($p < 1e\text{-}13$).

SEM pictures of BMBC samples coated with potassium stearate were not taken due to the expected one-molecule thick coating. A molecule of stearate has a hypothetical size of approximately 25 Å (D. S. Shrestha et al., 2008), which is smaller than the lowest possible resolution of a SEM.

3.1.1. ION EXCHANGE HYPOTHESIS

Immersion for 15 minutes yielded a significant increase in the mean contact angle compared to immersion for three seconds ($p < 0.05$ for all concentrations). Extended immersion also resulted in a more narrow distribution of WCA, pointing at a more uniform coating on BMBC's surface. Better hydrophobicity of the samples immersed for 15 minutes supports the hypothesis that stearate's adhesion to the material's surface is governed by an ion-exchange mechanism of potassium stearate in the solution to magnesium/calcium stearate on the surface.

In order to further investigate this hypothesis, stearate coating was applied to BC. By comparing the WCAs of BMBC to BC at equal stearate concentrations, it is possible to show whether the presence of the mineral crystals in BMBC contributes to the interaction between the material's surface and stearate anions. The stearate coating was applied by immersion for 15 minutes, and the results of the WCA measurements are shown in

Figure 3.2. The results show that BMBC has a significantly higher mean WCA ($p < 0.005$) for all stearate concentrations. These results, too, further corroborate the hypothesis. Implications hereof and possible ways to further investigate this matter are discussed in Chapter 4.

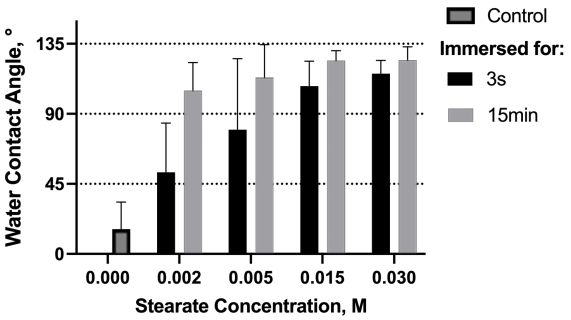

Figure 3.1: Water Contact Angle measurements for BMBC samples coated with potassium stearate of varying concentrations using different application methods: immersion into the solution for three seconds or fifteen minutes. Results for uncoated BMBC are also provided as a control.

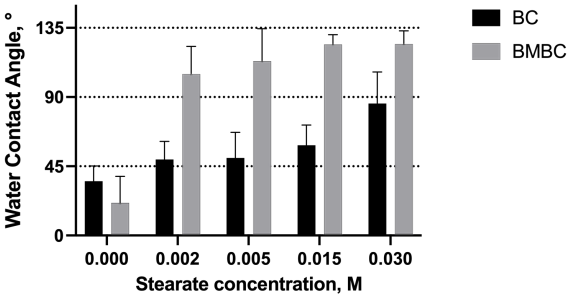

Figure 3.2: Water Contact Angle measurements for BMBC and BC samples coated with potassium stearate of varying concentrations.

3.1.2. ABRASION & WCA CHANGE AFTER 1 MINUTE

In order to test the robustness of the stearate coating, controlled abrasion was performed, using a setup described in Section 2.6. WCA was measured for the samples before and after abrasion; the results are shown in Figure 3.3. The samples experienced a significant ($p < 0.05$) drop in WCA for all stearate concentrations after the abrasion treatment.. A more significant standard deviation is also observed, pointing at the obtained irregularities in the coating caused by abrasion.

For lower concentrations of 0.002M and 0.005M, the post-abrasion mean WCA dropped to the negative control levels. For 0.015M the mean WCA dropped lower than 90°, meaning that the material qualitatively lost its hydrophobicity. However, despite the mean WCA for 0.03M staying above 90°, the high variance in WCA points to the lack of coating uniformity and, therefore, a loss of the surface's ability to resist water.

The results of the change in WCA from t=0s to t=60s are displayed in Figure 3.4. The only concentration at which the sample experienced a significant drop (23%) in WCA was 0.002M ($p < 1e\text{-}5$), meanwhile, all other concentrations did not experience a significant drop ($p \in [0.17; 0.39]$). This capacity of stearate coating to prevent water drops from seeping through corressponds with improved resistance to the wettability of BMBC and is further discussed in section 3.4, where the coated material's Water Absorption Capacity is reviewed.

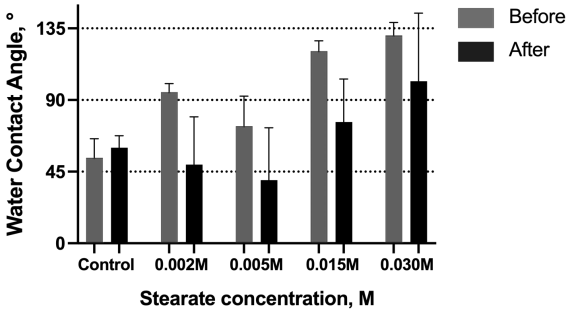

Figure 3.3: Water Contact Angle measurements for BMBC samples coated with potassium stearate of varying concentrations, performed before (dark gray) and after (black) controlled abrasion.

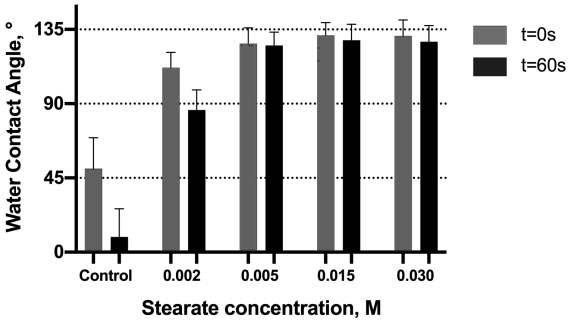

Figure 3.4: Water Contact Angle measurements for BMBC samples coated with potassium stearate of varying concentrations, performed directly after depositing a water drop on the surface (dark gray) and after 60 seconds (black).

3.2. CHITOSAN

As described in section 2.3.2, the orientation of the chitosan-coated sample during drying was imperative to the hydrophobicity, enhancing the ability of the coating. Figure 3.5 shows the results of WCA measurements for vertical drying and horizontal drying. Horizontal drying on a grid resulted in a significantly higher ($p < 1e\text{-}6$ for all concentrations) and more uniformly distributed WCA than vertical drying. A proposed clarification for this phenomenon is the slow flow of the highly viscous chitosan solution on the surface of BMBC to the lower side. This flow would result in a concentration gradient of chitosan on the surface, which would cause inconsistencies in the film formation during drying. In contrast, if dried horizontally, the gradient is more uniform, and a more homogeneous film forms on the surface.

However, it was expected that horizontal drying would lead to a difference in hydrophobicity between the two sides of the sample. Namely, the chitosan coating covering the "face-down" side experiences a gravitational pull, due to which some disturbance of the chitosan concentration gradient might occur. Despite this expectation, no significant difference was observed between the two sides ($p \in [0.20; 0.57]$), so in the continuation of this report, chitosan-coated samples were dried horizontally.

A peculiar observation from the graph in Figure 3.5 is that the chitosan concentration of 0.25% yielded the most significant increase in WCA ($p < 1e\text{-}18$) compared to the control. The mean WCA at 0.50% experiences a 14.2% drop ($p < 1e\text{-}4$), while at higher concentrations the mean doesn't change significantly ($p \in [0.18; 0.63]$). An explanation for this result was found upon examining the chitosan-coated samples with a SEM.

Figures 3.6a-3.6f display SEM micrographs of chitosan-coated BMBC samples' surfaces at varying concentrations. The most notable distinction is between the surface of BMBC at 0.25% chitosan and higher concentrations. In the concentration range above 0.25%, a smooth and thin film can be seen, covering the surface of BMBC, while at 0.25%, such film is not observed. The incidental cracks in the film, as seen in Figures 3.6c-3.6f, are presumably caused by the disturbances mentioned above in the chitosan gradient in the drying process. Moreover, the irregularities of the BMBC surface can cause an additional strain for film formation, as it is seen that the chitosan film is not tightly attached to the surface.

The hypothesis that a chitosan coating would provide the BMBC with a hydrophobic film does not apply to the 0.25% concentration, while this concentration also yields the highest mean WCA. A possible explanation for this is the formation of chitosan microstructures on the surface of BMBC, which causes an increase in the roughness of the material's surface. It is challenging to distinguish bacterial cellulose, PGA, and alginate from chitosan on a SEM picture, as all four appear as long fibers. It is, however, apparent that no chitosan film formation occurs at 0.25%, so further investigation is required to clarify the hydrophobicity-enhancing effect of the chitosan coating at this concentration.

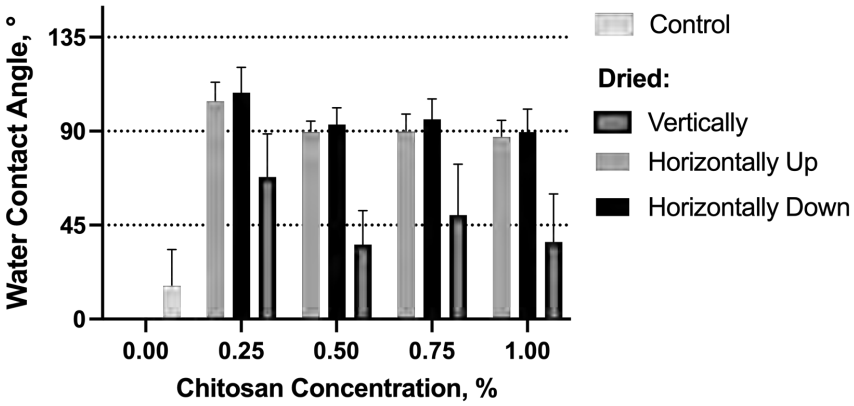

Figure 3.5: Water Contact Angle measurements for BMBC samples coated with chitosan of varying concentrations using different application methods: drying vertically or horizontally. Results for both the sides facing up and down are provided. Results for uncoated BMBC are also provided as a control.

3.2.1. ABRASION & WCA CHANGE AFTER 1 MINUTE.

The robustness of the chitosan coating was evaluated with controlled abrasion. The results depicted in Figure 3.7 show that the disturbance of the coating resulted in a loss of hydrophobicity ($p < 0.01$ for all concentrations), with the mean WCA decreasing even lower than the negative control. A potential explanation for the latter phenomenon is that, upon disturbance, the chitosan film causes more cracking in the BMBC's surface structure. Cracking the surface facilitates water seeping through, which could cause very low (<15°) WCA measurements.

However, the surface maintains some hydrophobicity, which can be seen in the increased variance of WCA. In fact, some local surface patches maintain hydrophobicity, which is tentatively caused by an undisturbed coating in those places.

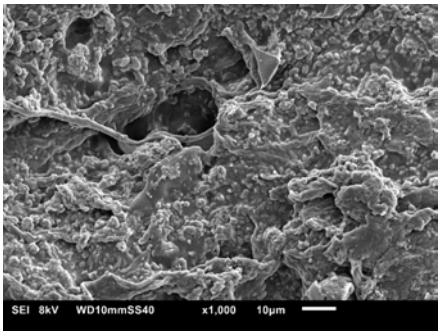

(a) SEM micrograph of a BMBC sample coated with 0.25% chitosan

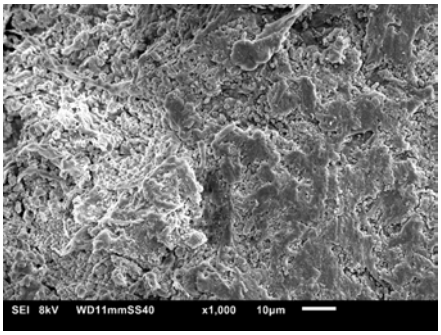

(b) SEM micrograph of an uncoated BMBC sample

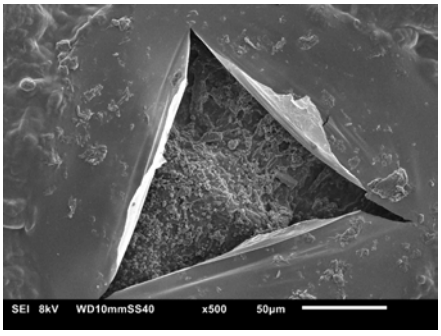

(c) SEM micrograph of a BMBC sample coated with 0.50% chitosan

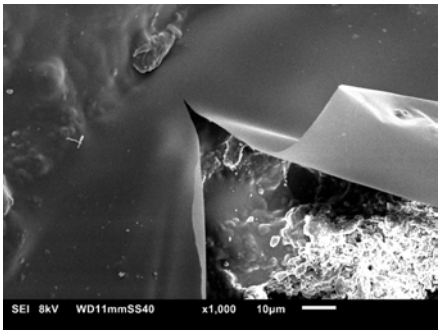

(d) SEM micrograph of a BMBC sample coated with 0.75% chitosan

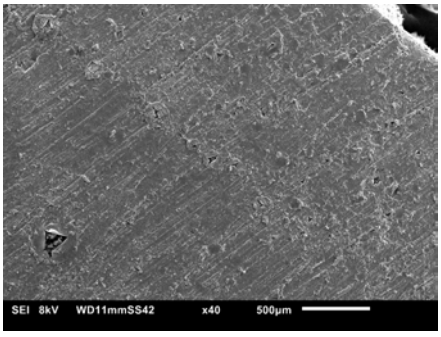

(e) SEM micrograph of a BMBC sample coated with 0.75% chitosan

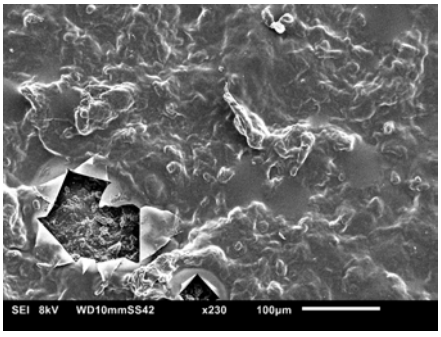

(f) SEM micrograph of a BMBC sample coated with 0.25% chitosan

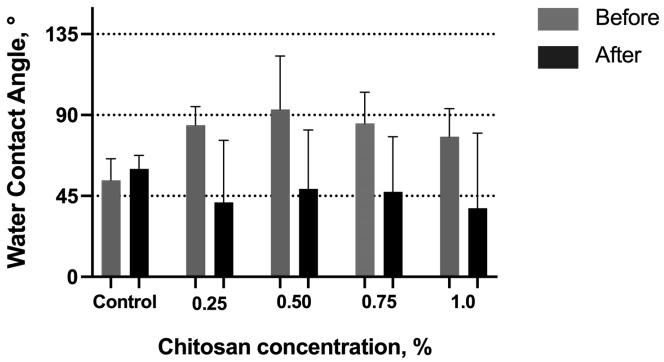

Figure 3.7: Water Contact Angle measurements for BMBC samples coated with chitosan of varying concentrations, performed before (dark gray) and after (black) controlled abrasion.

The one-minute WCA measurements for chitosan coating, as seen in Figure 3.8, show a significant decrease of 9-14% in the mean WCA for all concentrations ($p < 0.001$), except for 1.0%. The 4.2% drop in mean WCA at this concentration was not significant ($p = 0.158$). A plausible interpretation of this result is the increased uniformity of the formed film, which is achieved at higher concentrations of chitosan. A higher concentration leads to decreased sensitivity to gradient concentration fluctuations during film formation, which leads to minor cracking and, therefore, a more uniform coating. Such a consistent coating, in turn, results in a minimal decrease in mean WCA over the minute. The WAC measurements further support this clarification, as discussed in Section 3.4.

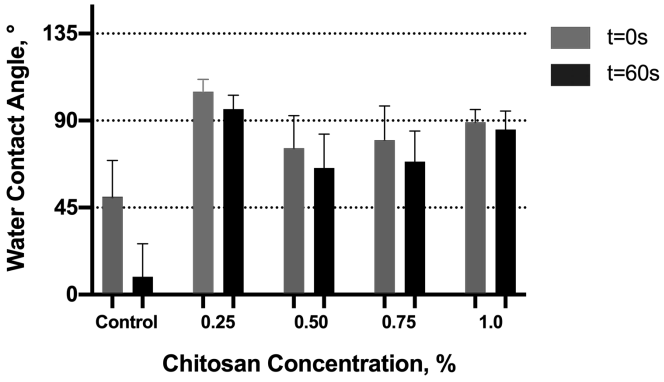

Figure 3.8: Water Contact Angle measurements for BMBC samples coated with chitosan of varying concentrations, performed directly after depositing a water drop on the surface (dark gray) and after 60 seconds (black).

3.2.2. CHITOSAN COMPOSITE

No results are shown for the formulated chitosan-BMBC composite material; however, some anecdotal evidence for WCA measurements corresponding with adequate hydrophobicity was obtained. During WCA measurements, some parts of the sample gave a WCA up to 95°. The 18 measurements gave a mean WCA of 34.3±40.6°, which yielded a p=0.09 compared to the negative control (15.9±17.0°). Additionally, the material appeared tougher and more brittle than BMBC without chitosan. Implications hereof are discussed in Chapter 4.

3.3. ZEIN

Similar to stearate and chitosan, the application of zein coating was performed with various methods in order to determine the most efficient. The comparison of WCA measurements for dry BMBC samples with or without soaking in ethanol prior to immersion in a zein solution is provided in Figure 3.9. Even though the change in the measurements was not convincingly significant (p = 0.155 for 0.5% and p = 0.054 for 5.0%), one-minute WCA and abrasion measurements were performed with soaked samples since the mean WCA was closer to 90°. The soaked samples yielded significantly higher WCA than the negative control (p < 1e-9), with the mean WCA being 88.4° for 0.5% and 78.3° for 5.0%.

Results for the third method, in which wet BMBC is immersed in ethanol for solvent exchange, after which it is placed in zein and finally dried, are not shown. The nature of this method relies on the formation of zein microstructures on the material's surface, which means that it must be air-dried. However, a flat BMBC sample must be obtained to conduct WCA measurements. The current protocol makes obtaining a flat BMBC sample when air-drying without applying any force impossible. Figure 3.9 shows optical images of a wet zein-coated BMBC sample before and after drying. It demonstrates that the sample shrinks substantially and that a flat surface cannot be obtained.

Moreover, the sample cannot be sandpapered to improve the surface's flatness, as it would destroy all the microstructures formed on the material's surface. Therefore, an alternative way to dry the material must be devised to employ this method to enhance the hydrophobicity of BMBC. This alternative method would require a more controlled way to dewater the sample, preventing unpredictable shrinkage.

Figures 3.11a-3.11d show SEM micrographs of the zein-coated samples. The primary distinction between the coating at 0.5% and 5.0% is the formation of the film. This phenomenon is similar to chitosan's behavior at increasing concentration, but no evident cracks were observed in the film at 5.0%. At 0.5%, peculiar flower-like microstructures can be observed (3.11a, 3.11b). These microstructures are irregularly distributed over the material's surface and appear as a very rough core with a diameter in the range of 4-7.5µm, occasionally with 3-6µm long petals or without them. A SEM micrograph of an uncoated sample is provided in Figure 3.11e to show that these flower-like microstructures are different from $CaCO_3$ or $MgCO_3$ round crystals present in BMBC. Notwithstanding that various microstructure shapes have been reported to form with zein molecules, no evidence for such shapes was found in the existing literature. Further research into the genesis and characterization of these microstructures is necessary to understand what their appearance can be attributed to.

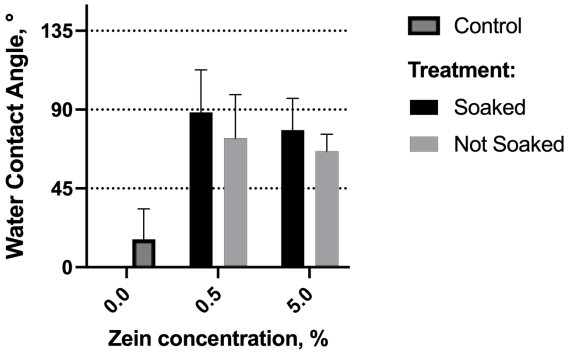

Figure 3.9: Water Contact Angle measurements for BMBC samples coated with zein of varying concentrations using different application methods: soaking a dry BMBC sample in ethanol for 24h prior to immersion in a zein solution or not. Results for uncoated BMBC are also provided as a control.

Figure 3.10: Optical images of a wet BMBC sample (left) next to a dried zein-coated BMBC sample (right). The left image depicts the samples from above, while the right image is a high-angle shot of the samples. The zein-coated sample was prepared according to the third protocol, as described in Section 2.3.

Despite the unclear character of the flower-like microstructures, they are expected to contribute to an increased roughness of the material's surface. Combined with the natural hydrophobicity of zein, this contributes to an enhanced surface hydrophobicity. At 5.0%, such microstructures are not observed, but very rough spheres without petals are present (3.11c, 3.11d). These could also contribute to the roughness of the surface and the hydrophobic zein film, which uniformly covers the surface of the material, provides consistency to this hydrophobicity. The thick fibrous film in the micrographs for 5.0% is consistent with the SEM pictures obtained in the paper by Wan et al., 2017, on which this methodology was based.

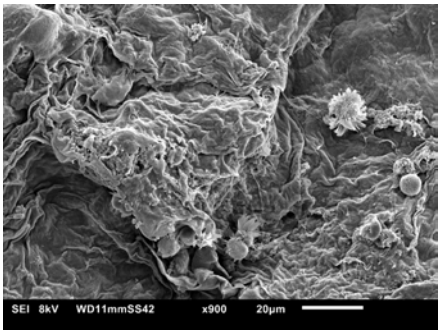

(a) SEM micrograph of a BMBC sample coated with 0.5% zein

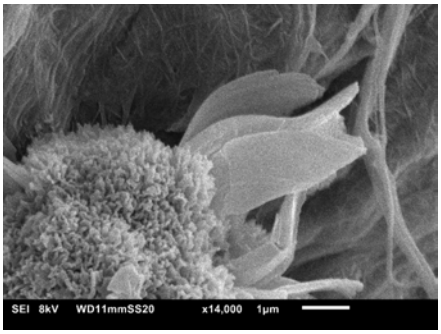

(b) SEM micrograph of a BMBC sample coated with 0.5% zein

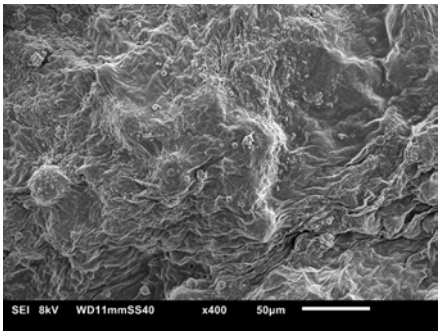

(c) SEM micrograph of a BMBC sample coated with 5.0% zein

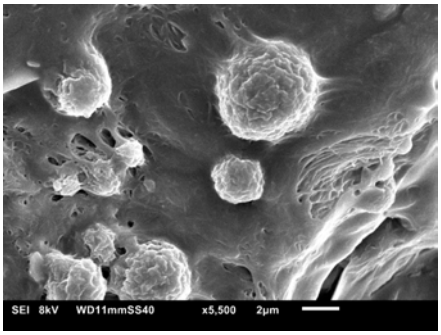

(d) SEM micrograph of a BMBC sample coated with 5.0% zein

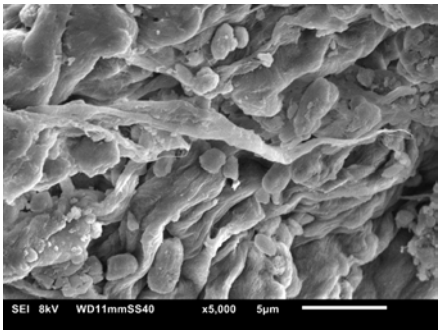

(e) SEM micrograph of an uncoated BMBC sample

3.3.1. ABRASION & WCA CHANGE AFTER 1 MINUTE.

Figure 3.13 shows the results of abrasion testing. As explained in the previous section, the hydrophobicity of the 0.5% sample is mainly attributed to the microstructures formed on the surface. In comparison, at 5.0%, a hydrophobic film is formed on the surface, which accounts for the enhanced hydrophobicity. Therefore, the microstructures are expected to be destroyed by abrasion, while the film should only partially be disturbed. The results in Figure 3.13 support this hypothesis. At 0.5%, abrasion causes a major drop in WCA to a mean of 8.4°, significantly lower than the mean WCA of the control sample ($p = 0.003$). This result is unexpected and should be further investigated, as the post-abrasion WCA is expected to be equal to that of the negative control. Namely, abrasive treatment is not expected to improve the surface's hydrophilicity since the material's morphology remains unchanged. For 5.0%, WCA decreased to a mean of 63.4°, which is not significantly higher than the 60.6° mean WCA of negative control ($p = 0.37$), signifying the loss of hydrophobicity of the BMBC surface upon abrasion.

Figure 3.12 displays the results for one-minute WCA measurements. For both 0.50% ($p = 0.026$ when WCA at t=60s is compared to WCA at t=0s) and 5.0% ($p < 1e\text{-}3$ when WCA at t=60s is compared to WCA at t=0s) mean WCA significantly decreases with approximately 20%. This performance is worse than the other two coatings. It can be attributed to the lack of uniformity of the zein coating due to the lack of control in the evaporation-induced microstructure formation during air-drying.

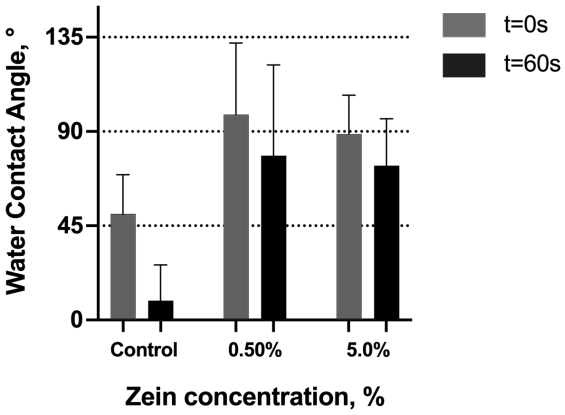

Figure 3.12: Water Contact Angle measurements for BMBC samples coated with zein of varying concentrations, performed before (dark gray) and after (black) controlled abrasion.

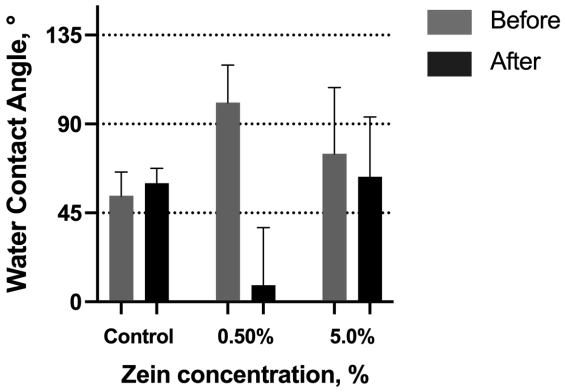

Figure 3.13: Water Contact Angle measurements for BMBC samples coated with zein of varying concentrations, performed directly after depositing a water drop on the surface (dark gray) and after 60 seconds (black).

3.4. CROSS-COMPARISON

This section compares the three applied coatings by plotting the results obtained for the three WCA measurements for an ostensive overview. Besides the cross-comparison of the WCA measurements, WAC and drop absorption graphs are provided.

3.4.1. WATER CONTACT ANGLE MEASUREMENTS

In order to evaluate the three coatings' hydrophobicity enhancing capacity, Figure 3.14 and Tables 3.1 and 3.2 were set up to summarize the data from the graphs shown in previous sections. Figure 3.14 shows WCA for all the tried coatings at various concentrations, as well as with various methods of application. It appears that coating with 0.03M stearate yields the highest WCA, while among the other coatings, only the 0.25% chitosan coating attains the desired WCA of 90°. WCA of the stearate coating increases with an increasing concentration, which points to the possibility of attaining an even better hydrophobicity at higher concentrations.

Table 3.1 shows the decrease of WCA before and after abrasion in percent, in which 0.03M stearate also shows the best robustness (5.0% zein gives a mean WCA value after abrasion that is almost equal to that of the negative control). An increasing stearate concentration shows an increasingly better performance here, too. Only 0.03M stearate can maintain hydrophobicity (WCA > 90°) after abrasion.

Table 3.2 shows one-minute WCA measurements for all coated samples. Stearate coating with concentrations above 0.002M performs best for this test. Chitosan also displays sufficient capacity to prevent the water drop from seeping through the coating. Zein at 0.5% shows a great variance, pointing at the scarce uniformity of the formed coating. The film that forms at 5.0% performs similarly to the chitosan film coatings.

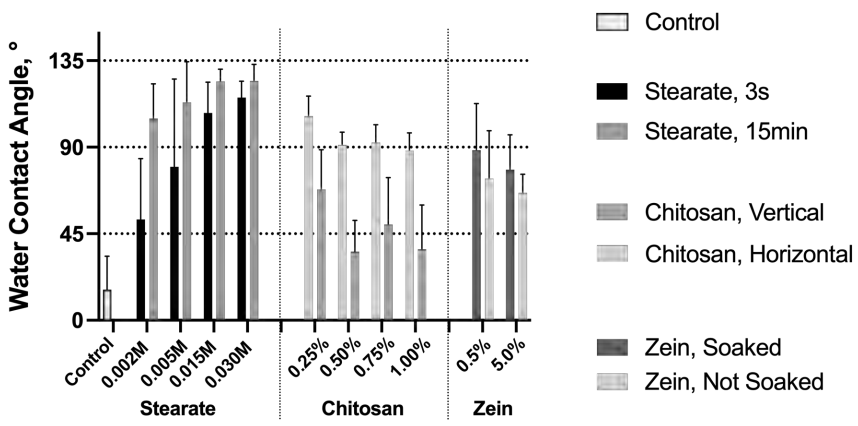

Figure 3.14: Water Contact Angle measurements for BMBC samples coated with stearate, chitosan and zein at varying concentrations and different methods of application.

Table 3.1: A summary of results of WCA measurements before and after abrasion for BMBC samples coated with stearate, chitosan and zein at varying concentrations.

Coating	**Concentration**	**Mean WCA before abrasion**	**Mean WCA after abrasion**	$\frac{\text{Mean WCA after abrasion}}{\text{Mean WCA before abrasion}}$, %
Control		60.0°	53.7°	111.74%
Stearate	0.002M	94.9°	49.4°	52.03%
	0.005M	73.6°	39.7°	54.00%
	0.015M	120.6°	76.1°	63.11%
	0.03M	130.6°	101.8°	77.93%
Chitosan	0.25%	41.5°	84.4°	49.19%
	0.50%	93.0°	48.9°	52.58%
	0.75%	85.3°	47.3°	55.42%
	1.0%	78.0°	38.2°	49.02%
Zein	0.5%	100.8°	8.4°	8.35%
	5.0%	75.0°	63.4°	84.52%

Table 3.2: A summary of results of one-minute WCA measurements for BMBC samples coated with stearate, chitosan and zein at varying concentrations.

Coating	Concentration	Mean WCA at t=0s	Mean WCA at t=60s	$\frac{\text{WCA at t=60s}}{\text{WCA at t=0s}}$, %
Control		50.6°	9.2°	17.51% ± 33.09%
Stearate	0.002M	111.9°	86.2°	77.24% ± 10.06%
	0.005M	126.4°	125.3°	104.28% ± 10.06%
	0.015M	131.4°	128.5°	102.94% ± 12.54%
	0.03M	131.1°	127.5°	97.30% ± 3.32%
Chitosan	0.25%	104.9°	95.9°	91.55% ± 6.12%
	0.50%	75.7°	65.5°	86.02% ± 7.87%
	0.75%	80.0°	68.8°	86.30% ± 8.67%
	1.0%	89.1°	85.4°	95.97% ± 9.83%
Zein	0.5%	98.1°	78.5°	71.13% ± 37.32%
	5.0%	88.8°	73.7°	82.43% ± 12.84%

3.4.2. WATER ABSORPTION CAPACITY MEASUREMENTS

Finally, to evaluate the water-resistant properties of the coated samples, WAC measurements were performed over one hour and after 24h. WAC represents the ability of the coating to prevent wetting and water absorption when the sample is fully immersed in water. The results of these measurements are shown in Figure 3.16. The plot shows a more significant distribution of the WAC in the first thirty minutes, after which it converges towards the negative control measurements. A pairwise Tukey test was used to identify samples with a significantly lower mean WAC value than the negative control at the different intervals.

After five minutes, 1.0% chitosan coating showed a 22% lower mean WAC than the control ($p = 0.008$). After 15 minutes, which also appears to be the time point with the highest variance in WAC, chitosan coatings at 0.25%, 0.50%, and 1.0% all had a significantly lower mean ($p < 0.005$). 0.25% and 0.50% gave a 14-16% lower mean WAC value, while 1.0% led to a decrease in the mean WAC of 40%. At 30 minutes, only 1.0% had a significantly lower mean with 21% ($p = 0.05$). Since the 15-minute time point had the highest mean WAC variance, the WAC at this time point is displayed in Figure 3.17 as a bar plot for a greater visual resolution.

Another metric used to quantify the coating's capacity to improve the wettability of the BMBC sample is Water Drop Absorption. During the experiments, it became evident that most coatings were not homogeneous enough to ensure robust sample encapsulation.

Therefore, when a water drop is placed on the surface of the sample, it starts slowly seeping through. The time it takes for a drop of water to disappear from the material's surface by either seeping through or evaporating was recorded. The theoretical value for evaporation of a water drop of $6\mu L$ was calculated, as explained in Appendix A. This value amounted to 69.4min, which roughly corresponds to the maximum value obtained for stearate: 72.5min. This correspondence points to the fact that the water drop did not seep through the stearate coating but instead evaporated.

The results are displayed in Figure 3.15. For this test, all coatings except for 0.25% chitosan and 5.0% zein yielded significantly better performance ($p < 0.05$) than the control. The performance of the different coatings for this test is put into context in Chapter 4.

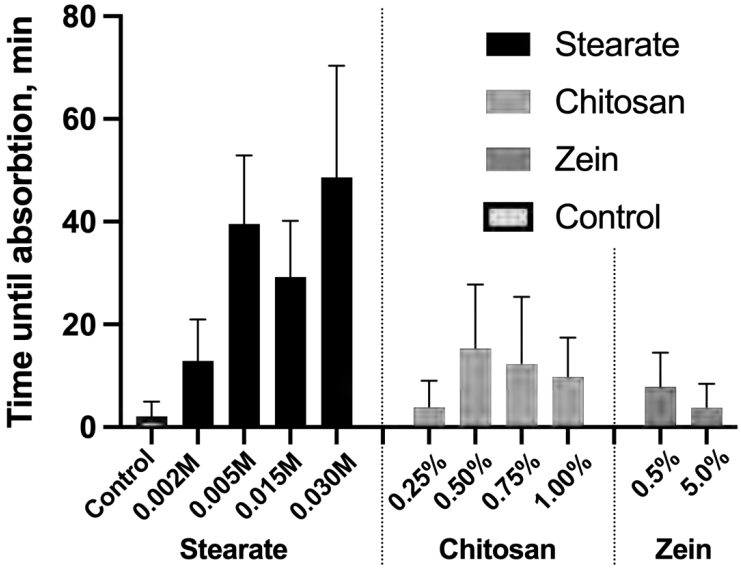

Figure 3.15: Drop Absorption measurements for BMBC samples coated with stearate, chitosan and zein at varying concentrations. Methods of coating application are: 15 minute immersion; horizontal drying and soaked in ethanol.

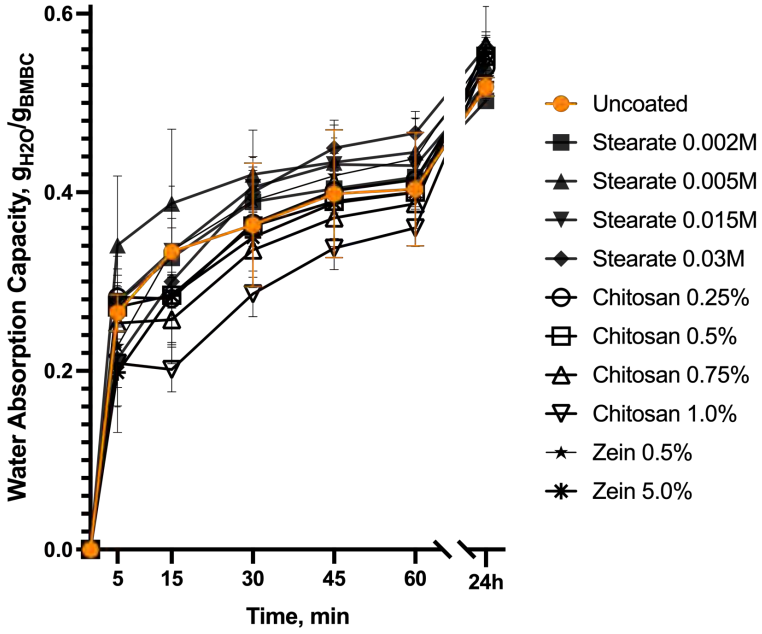

Figure 3.16: Water Absorption Capacity measurements for BMBC samples coated with stearate, chitosan and zein at varying concentrations. In the first hour the mass measurements are taken at 5, 15, 30, 45, 60 minutes, then after 24h. Methods of coating application are: 15 minute immersion; horizontal drying and soaked in ethanol.

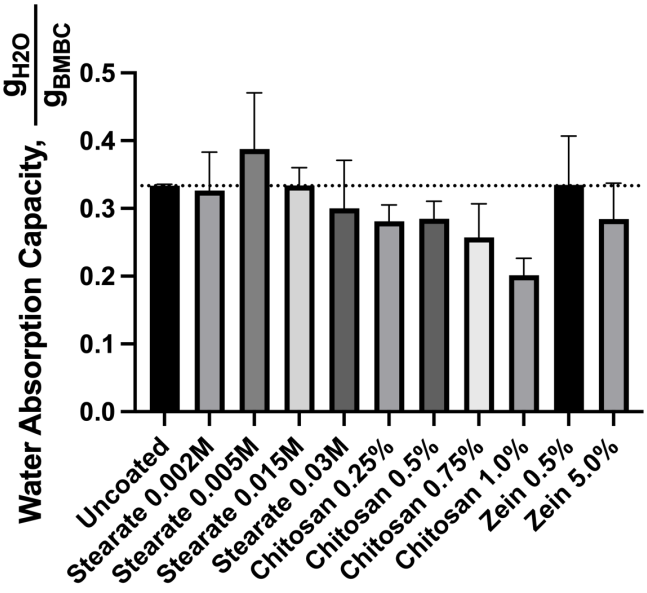

Figure 3.17: Water Absorption Capacity measurements at t = 15min for BMBC samples coated with stearate, chitosan and zein at varying concentrations. Methods of coating application are: 15 minute immersion; horizontal drying and soaked in ethanol.

4

Discussion & Conclusion

In the frame of this project, three coatings were examined on their capacity to enhance the water-resistance of BMBC: potassium stearate, chitosan, and zein. Several metrics were used to assess the water-resistance of the coated BMBC samples, mainly focusing on the surface wettability, water absorption, and coating robustness. WCA measurements were used to evaluate the surface wettability; WAC and drop absorption measurements were used to analyze water absorption; controlled abrasion was performed to characterize the coating robustness.

Several methods of applying the coatings were assayed to devise an optimal protocol. Firstly, potassium stearate coating showed better results in the WCA measurements when the BMBC sample was immersed in the solution for 15 minutes rather than for three seconds. Secondly, better results were obtained for the chitosan coating when the coated samples were horizontally dried, while both sides yielded equally high WCA. Finally, zein gave better results for WCA when a dry BMBC sample was soaked in ethanol before immersion into zein. These results serve as the first steps in devising an optimal protocol for BMBC coating to achieve enhanced hydrophobicity.

The first part of the assays included Water Contact Angle measurements of the coated samples, along with a one-minute WCA reduction and before-and-after abrasion WCA reduction assays. While all coatings resulted in a significant mean WCA for the standard measurements, only some coatings gave a WCA >90°, which is typically the threshold for claiming hydrophobicity of a surface. The surface yielded a WCA of more than 90° for stearate coating at all concentrations, chitosan coating at 0.25%, 0.5%, and 0.75%, while zein failed to provide sufficient hydrophobicity. These results are summarized in Figure 3.14.

Potassium stearate coatings also performed best for the one-minute and abrasion WCA measurements, especially at higher concentrations. This trend for a better performance of a stearate coating at an increasing concentration was observed for all measurements, including drop absorption. This result points to the possibility of expanding the concentration range of the applied stearate coating to achieve even better robustness and hydrophobicity of the stearate coating.

However, the trend for improving the wettability resistance of increasingly concentrated stearate coatings did not apply to the second part of the performed assays, the WAC measurements. Namely, no significant improvement in preventing water absorption by a BMBC sample was obtained when coated with stearate. This poor performance in preventing water absorption raises a question about the optimality of dip/immersion coating when applied to BMBC.

Firstly, the current protocol for formulating samples of BMBC is not optimized for obtaining flat samples, which leads to the formation of highly porous and uneven surfaces when dried. Sometimes the obtained samples are so uneven that even thorough sandpapering does not provide sufficient flatness. Furthermore, when the samples are not flat before applying the coating, this could result in film cracking, as with chitosan or zein, or in the non-homogeneous distribution of surface-grafted stearate molecules on the surface. These features result in disturbed or unevenly distributed water-resistant properties of the coated samples, which results in inconsistent WCA measurements and poor performance in preventing water absorption since irregularities in the coating enable water to seep through the coating. This shortcoming of the current BMBC sample formulation protocol should be addressed if a more consistent methodology for any coating for BMBC is to be devised.

One of the possible alternatives to the current formulation protocol is using a controlled sheet former, as in Wan et al., 2017, or a controlled sand-blower to polish the surfaces of BMBC before coating.

Secondly, an optimization of stearate immersion duration and stearate concentration is necessary. Such optimization should be done with such features as sample swelling and achieved water resistance.

Thirdly, the ion exchange mechanism should be elucidated to claim whether stearate has the highest affinity to MgCO3 and CaCO3 in BMBC. Then, perhaps, a different salt of stearate, e.g., sodium, will be more efficient in facilitating the ion exchange with the mineral crystals in BMBC, which would improve the water-resistant enhancing properties of the applied stearate coating. In general, this capacity of employing an ion-exchange mechanism for surface grafting of BMBC is an attractive topic for further investigation.

Besides stearate coating, chitosan and zein coatings also experience sub-optimal performance, which can be attributed to the mode of application of the chosen coating, as well as the structure of BMBC's surface. As seen in Figures 3.11d and 3.6a, the uneven nature of the BMBC surface causes disturbances in the formulated coatings. These disturbances, in turn, lead to poor performance in protecting the material against water absorption, which is detrimental to the water-resistant performance of the coated samples.

Both zein and chitosan coatings show promising surface hydrophobicity, which points to the potential to optimize the concentration or application method of the used coatings to devise a method that would yield a coating that could be more efficient and robust. Furthermore, the transition from increased roughness to forming a hydrophobic film on the material's surface is particularly interesting for both coatings. If optimized, an optimum between surface roughness and film formation could be found, which would further the cause of the application of bio-based biodegradable coatings for enhancing hydrophobicity for a multitude of materials.

Even though this project only superficially regarded zein, it showed some potential in water-resistant enhancing properties. Therefore, more detailed research is demanded to integrate a zein coating into the formulation of a BMBC material sample. Since the study by Wan et al., 2017, on which zein coating was based, also used hot pressing to create a BC-zein composite with increased surface roughness, a more detailed study of various techniques to create zein-BMBC composites is required to make a well-founded statement on the efficiency and robustness of this coating.

Complementary to this, thorough research into the genesis of the flower-like microstructures, as seen in Figure 3.11a is required to understand the interaction of zein with the compounds in BMBC. Elucidating the origin of these microstructures would contribute to the application of zein for enhancing the hydrophobicity of BMBC. Moreover, it would expand the field of microstructures that zein can form under evaporation-induced conditions.

Another briefly discussed technique to enhance the water-resistant capacity of the BMBC coating is the formulation of a chitosan composite. Even though a statistically significant increase in WCA was not achieved ($p = 0.09$), the occasional occurrence of WCA > 90° point to the potential of optimizing this method to tweak the properties of BMBC. Although mechanical properties were not assessed, the empirical tactile assessment signified an increase in material toughness. This capacity of BMBC properties to be tweaked by the addition of other molecules during biomineralization is also an attractive feature of the studied material. Therefore, further research is necessary into the different material formulations for tweaking the mechanical and physical properties of the material.

Nonetheless, the results of the WCA measurements from the pre- and post-abrasion, as seen in Figure 3.1 emphasize the significant shortcomings of film-forming coatings. When disrupted, film coatings experience a significant drop in resistance to wettability and absorption. For the furniture and stationery applications proposed in the paper by Yu et al., 2021, such poor performance upon disruption is undesired. Therefore, stearate coating appears to be most promising for BMBC.

In order to further the efforts of this project, some aspects of the studied coatings should be elaborated on. First, ion exchange with the CaCO3 and MgCO3 crystals is a potentially interesting tool that can be utilized for surface grafting of BMBC. Furthermore, fatty acids, as well as other molecules of ionic nature, can be employed for tweaking the physical properties. Second, to achieve more reproducible and effective results in coating BMBC, researchers are advised to optimize the protocol for dewatering BMBC to achieve a more predictable surface morphology. This would alleviate the irregularities that might cause the film coatings to break. Lastly, incorporating other molecules in the biomineralization process seems like an auspicious method of tuning the material properties of BMBC.

To conclude, BMBC is a promising bio-based material with attractive mechanical properties but less advantageous physical properties. Further research into tweaking physical properties is required to achieve the appropriate tuneability for desired applications.

APPENDICES

:

A. CALCULATION OF THEORETICAL EVAPORATION RATE OF A WATER DROP

The formula for empirical evaporation rate of a water drop from a surface was obtained from Engineering Toolbox, 2004:

$$g_h = (25 + 19v) * A * (X_s - X), \text{ where}$$

g_h = amount of evaporated water per hour (kg/h)
v = velocity of air above the water surface (m/s)
A = water surface area (m2)
X_s = maximum humidity ratio of saturated air at the same temperature as the water surface (kg/kg) (kg H2O in kg Dry Air)
X = humidity ratio air (kg/kg) (kg H2O in kg Dry Air)

Tabular values were taken for T=20°C and pressure of p=1atm. This gives $X_s = 0.014659 kg_{water}/kg_{air}$ and $X = 0.014659 kg_{water}/kg_{\text{dry air}}$ using the ideal gas law. The evaporation surface area was approximated by the area of a sphere, with the known volume of the drop of water on the surface of $6\mu L$. Then with $V = \frac{4}{3}\pi r^3$ the radius is calculated (r=1.127e-3) and this is plugged into $A = 4\pi r^2$, giving A= 1.596e-5. Velocity of air above the water surface is set to 0m/s.

This gives g_h = (25+19*0)*1.596e-5*(0.014659-0.0098)=5.189e-5 kg/s. The mass of the drop is 6.0e-9m^3*100kg/m^3=6.0e-6kg, which gives an evaporation time of 6.0e-6kg / 5.189e-5kg/h = 1.156h = 69.37min.

BIBLIOGRAPHY

Andreotti, S., Franzoni, E., Degli Esposti, M., & Fabbri, P. (2018). Poly(hydroxyalkanoate)s-Based Hydrophobic Coatings for the Protection of Stone in Cultural Heritage. *Materials*, *11*(1), 165. https://doi.org/10.3390/ma11010165

Belgacem, M., & Gandini, A. (2008). *Monomers, Polymers and Composites from Renewable Resources*. Elsevier Gezondheidszorg.

Bhushan, B., Jung, Y. C., & Koch, K. (2009). Self-Cleaning Efficiency of Artificial Superhydrophobic Surfaces. *Langmuir*, *25*(5), 3240–3248. https://doi.org/10.1021/la803860d

Brugnara, M. (2006). Contact Angle ImageJ Plugin.

Cabañas-Romero, L. V., Valls, C., Valenzuela, S. V., Roncero, M. B., Pastor, F. I. J., Diaz, P., & Martínez, J. (2020). Bacterial Cellulose–Chitosan Paper with Antimicrobial and Antioxidant Activities. *Biomacromolecules*, *21*(4), 1568–1577. https://doi.org/10.1021/acs.biomac.0c00127

Cheng, Q.-Y., An, X.-P., Li, Y.-D., Huang, C.-L., & Zeng, J.-B. (2017). Sustainable and Biodegradable Superhydrophobic Coating from Epoxidized Soybean Oil and ZnO Nanoparticles on Cellulosic Substrates for Efficient Oil/Water Separation. *ACS Sustainable Chemistry & Engineering*, *5*(12), 11440–11450. https://doi.org/10.1021/acssuschemeng.7b02549

Coherent Marketing Insights. (2019). Stearates Market Size, Trends And Forecast To 2027. https://www.coherentmarketinsights.com/insight/stearates-market-4131/toc

D. S. Shrestha, J. Van Gerpen, & J. Thompson. (2008). Effectiveness of Cold Flow Additives on Various Biodiesels, Diesel, and Their Blends. *Transactions of the ASABE*, *51*(4), 1365–1370. https://doi.org/10.13031/2013.25219

Dong, F., Padua, G. W., & Wang, Y. (2013). Controlled formation of hydrophobic surfaces by self-assembly of an amphiphilic natural protein from aqueous solutions. *Soft Matter*, *9*(25), 5933. https://doi.org/10.1039/c3sm50667c

Dong, X., Gao, S., Huang, J., Li, S., Zhu, T., Cheng, Y., Zhao, Y., Chen, Z., & Lai, Y. (2019). A self-roughened and biodegradable superhydrophobic coating with UV shielding, solar-induced self-healing and versatile oil–water separation ability. *Journal of Materials Chemistry A*, *7*(5), 2122–2128. https://doi.org/10.1039/C8TA10869B

Engineering Toolbox. (2004). Evaporation from a Water Surface. 28/06/2022https://www.engineeringtoolbox.com/evaporation-water-surface-d_690.html

Ensikat, H. J., Ditsche-Kuru, P., Neinhuis, C., & Barthlott, W. (2011). Superhydrophobicity in perfection: the outstanding properties of the lotus leaf. *Beilstein Journal of Nanotechnology*, *2*, 152–161. https://doi.org/10.3762/bjnano.2.19

Fernandes, S. C. M., Oliveira, L., Freire, C. S. R., Silvestre, A. J. D., Neto, C. P., Gandini, A., & Desbriéres, J. (2009). Novel transparent nanocomposite films based on chitosan and bacterial cellulose. *Green Chemistry*, *11*(12), 2023. https://doi.org/10.1039/b919112g

Fürstner, R., Barthlott, W., Neinhuis, C., & Walzel, P. (2005). Wetting and Self-Cleaning Properties of Artificial Superhydrophobic Surfaces. *Langmuir*, *21*(3), 956–961. https://doi.org/10.1021/la0401011

Gianazza, E., Viglienghi, V., Righetti, P. G., Salamini, F., & Soave, C. (1977). Amino acid composition of zein molecular components. *Phytochemistry*, *16*(3), 315–317. https://doi.org/10.1016/0031-9422(77)80054-X

Hahn, T., Bossog, L., Hager, T., Wunderlich, W., Breier, R., Stegmaier, T., & Zibek, S. (2019). Chitosan Application in Textile Processing and Fabric Coating. *Chitin and chitosan* (pp. 395–428). Wiley. https://doi.org/10.1002/9781119450467.ch16

Hu, Z., Zen, X., Gong, J., & Deng, Y. (2009). Water resistance improvement of paper by superhydrophobic modification with microsized CaCO3 and fatty acid coating. *Colloids and Surfaces A: Physicochemical and Engineering Aspects*, *351*(1-3), 65–70. https://doi.org/10.1016/j.colsurfa.2009.09.036

Huang, T., Li, K. D., & Ek, M. (2021). Hydrophobization of cellulose oxalate using oleic acid in a catalyst-free esterification suitable for preparing reinforcement in polymeric composites. *Carbohydrate Polymers*, *257*, 117615. https://doi.org/10.1016/j.carbpol.2021.117615

Indriyati, Frecilla, N., Nuryadin, B. W., Irmawati, Y., & Srikandace, Y. (2020). Enhanced Hydrophobicity and Elasticity of Bacterial Cellulose Films by Addition of Beeswax. *Macromolecular Symposia*, *391*(1), 1900174. https://doi.org/10.1002/masy.201900174

Ivanova, N., & Philipchenko, A. (2012). Superhydrophobic chitosan-based coatings for textile processing. *Applied Surface Science*, *263*, 783–787. https://doi.org/10.1016/j.apsusc.2012.09.173

Ji-Suk Jeong. (2012). Water absorption and maintenance of nanofiber cellulose production by Gluconacetobacter rhaeticus TL-2C. *AFRICAN JOURNAL OF BIOTECHNOLOGY*, *11*(40). https://doi.org/10.5897/AJB11.3034

Kansal, D., Hamdani, S. S., Ping, R., & Rabnawaz, M. (2020). Starch and Zein Biopolymers as a Sustainable Replacement for PFAS, Silicone Oil, and Plastic-Coated Paper. *Industrial & Engineering Chemistry Research*, *59*(26), 12075–12084. https://doi.org/10.1021/acs.iecr.0c01291

Liu, Y., Liu, Z., Liu, Y., Hu, H., Li, Y., Yan, P., Yu, B., & Zhou, F. (2015). One-Step Modification of Fabrics with Bioinspired Polydopamine@Octadecylamine Nanocapsules for Robust and Healable Self-Cleaning Performance. *Small*, *11*(4), 426–431. https://doi.org/10.1002/smll.201402383

Mohanty, A. K., Vivekanandhan, S., Pin, J.-M., & Misra, M. (2018). Composites from renewable and sustainable resources: Challenges and innovations. *Science*, *362*(6414), 536–542. https://doi.org/10.1126/science.aat9072

Nakajima, A., Hashimoto, K., Watanabe, T., Takai, K., Yamauchi, G., & Fujishima, A. (2000). Transparent Superhydrophobic Thin Films with Self-Cleaning Properties. *Langmuir*, *16*(17), 7044–7047. https://doi.org/10.1021/la000155k

Nimittrakoolchai, O.-U., & Supothina, S. (2008). Deposition of organic-based superhydrophobic films for anti-adhesion and self-cleaning applications. *Journal of the European Ceramic Society*, *28*(5), 947–952. https://doi.org/10.1016/j.jeurceramsoc.2007.09.025

Nyström, D., Lindqvist, J., Östmark, E., Antoni, P., Carlmark, A., Hult, A., & Malmström, E. (2009). Superhydrophobic and Self-Cleaning Bio-Fiber Surfaces via ATRP and Subsequent Postfunctionalization. *ACS Applied Materials & Interfaces*, *1*(4), 816–823. https://doi.org/10.1021/am800235e

Pardo-Castaño, C., & Bolaños, G. (2019). Solubility of chitosan in aqueous acetic acid and pressurized carbon dioxide-water: Experimental equilibrium and solubilization

kinetics. *The Journal of Supercritical Fluids*, *151*, 63–74. https://doi.org/10.1016/j.supflu.2019.05.007

Schneider, C. A., Rasband, W. S., & Eliceiri, K. W. (2012). NIH Image to ImageJ: 25 years of image analysis. *Nature Methods*, *9*(7), 671–675. https://doi.org/10.1038/nmeth.2089

Seabold, S., & Perktold, J. (2010). statsmodels: Econometric and statistical modeling with python. *9th Python in Science Conference*.

Song, J., & Rojas, O. J. (2013). PAPER CHEMISTRY: Approaching super-hydrophobicity from cellulosic materials: A Review. *Nordic Pulp & Paper Research Journal*, *28*(2), 216–238. https://doi.org/10.3183/npprj-2013-28-02-p216-238

United Nations. (2020). Sustainable consumption and production. https://www.un.org/sustainabledevelopment/sustainable-consumption-production/

Veigel, S., Lems, E.-M., Grüll, G., Hansmann, C., Rosenau, T., Zimmermann, T., & Gindl-Altmutter, W. (2017). Simple Green Route to Performance Improvement of Fully Bio-Based Linseed Oil Coating Using Nanofibrillated Cellulose. *Polymers*, *9*(12), 425. https://doi.org/10.3390/polym9090425

Virtanen, P., Gommers, R., Oliphant, T. E., Haberland, M., Reddy, T., Cournapeau, D., Burovski, E., Peterson, P., Weckesser, W., Bright, J., van der Walt, S. J., Brett, M., Wilson, J., Millman, K. J., Mayorov, N., Nelson, A. R. J., Jones, E., Kern, R., Larson, E., … Vázquez-Baeza, Y. (2020). SciPy 1.0: fundamental algorithms for scientific computing in Python. *Nature Methods*, *17*(3), 261–272. https://doi.org/10.1038/s41592-019-0686-2

Wan, Z., Wang, L., Ma, L., Sun, Y., & Yang, X. (2017). Controlled Hydrophobic Biosurface of Bacterial Cellulose Nanofibers through Self-Assembly of Natural Zein Protein. *ACS Biomaterials Science and Engineering*, *3*(8), 1595–1604. https://doi.org/10.1021/ACSBIOMATERIALS.7B00116/ASSET/IMAGES/LARGE/AB-2017-00116W{_}0009.JPEG

Yilmaz Atay, H. (2019). Antibacterial Activity of Chitosan-Based Systems. *Functional chitosan* (pp. 457–489). Springer Singapore. https://doi.org/10.1007/978-981-15-0263-7{_}15

Yu, K., Spiesz, E. M., Balasubramanian, S., Schmieden, D. T., Meyer, A. S., & Aubin-Tam, M. E. (2021). Scalable bacterial production of moldable and recyclable biomineralized cellulose with tunable mechanical properties. *Cell Reports Physical Science*, *2*(6). https://doi.org/10.1016/j.xcrp.2021.100464

Zeng, W., Chen, J., Yang, H., Deng, L., Liao, G., & Xu, Z. (2017). Robust coating with superhydrophobic and self-cleaning properties in either air or oil based on natural zeolite. *Surface and Coatings Technology*, *309*, 1045–1051. https://doi.org/10.1016/j.surfcoat.2016.10.036

Zhu, Y., Romain, C., & Williams, C. K. (2016). Sustainable polymers from renewable resources. *Nature*, *540*(7633), 354–362. https://doi.org/10.1038/nature21001

ACKNOWLEDGEMENTS

I would like to thank all members of the Aubin-Tam group for accommodating me as an equal member for the last four months. For me, this project was dedicated not only to expanding my skillset or contributing to the ongoing research but also to seeing what kind of exciting stuff is being done outside the regular curriculum of the Life Science & Technology program. Bionanoscience served me well in this regard, as I saw a variety of people working on subjects outside of my comfort zone. In our conversations, I felt intellectually challenged, which made me excited. In turn, this excitement helped me understand the ways of science and my goals for the coming years more profoundly.

First, I would like to thank Ingo Nettersheim for daily supervision, teaching me the craft of taming bacteria and the art of fermentation, and the countless productive and fun conversations we shared.

Secondly, I would like to express gratitude to Roland Kieffer. His crazy gadgets and creative outlook on problem-solving akin to a true engineer, helped me solve severe bottlenecks in my project.

Thirdly, I would like to thank Ramon van der Valk, whose patient and understanding approach to conducting lab work provided me with a safe feeling at all times.

Lastly, I would like to thank Marie-Eve Aubin-Tam for her clear-eyed guidance. Our weekly discussions were always saturated with a profound feeling of experience and wisdom, which consistently reassured me. I am very grateful for her trust in me to conduct a very independent project. This opportunity gave me a feeling of pride and engagement with the project that was truly my own- which is rarely the case for a bachelor thesis.

All these people ensured that the four months I had spent sharing a lab with them were educational, fun, and engaging. I have learned a lot, and this could not have been without you all. Thank you very much.